Optimal Sizing and Siting of Fresh and Second-Life Battery Energy Storage Systems Based on Linearized Optimal Power Flow for High Photovoltaic Penetration: A Comparative Study

Chico Hermanu Brillianto Apribowo[1,2], Sasongko Pramono Hadi[1], F. Danang Wijaya[1], Sarjiya[1,3,*]

[1]Department of Electrical and Information Engineering, Universitas Gadjah Mada, Yogyakarta 55281, Indonesia

[2]Department of Electrical Engineering, Universitas Sebelas Maret, Surakarta 57126, Indonesia

[3]Center for Energy Studies, Universitas Gadjah Mada, Yogyakarta 55281, Indonesia

*Author to whom correspondence should be addressed:
E-mail: sarjiya@ugm.ac.id

(Received December 4, 2023: Revised April 16, 2024: Accepted June 21, 2024).

Abstract: The optimization of battery energy storage systems (BESS) is becoming increasingly popular among consumers due to numerous advantages, such as improved energy efficiency, cost-effectiveness, and promotion of network stability. As electric vehicle (EV) battery ages, effective management is essential after the removal of battery to improve energy efficiency. In this context, repurposing second-life battery (SLB) for BESS applications provides a highly attractive alternative to direct recycling or disposal, offering both economic and environmental benefits. Therefore, this study aimed to determine optimal sizing and siting of BESS by comparing both fresh battery and SLB in the IEEE 14 bus. The analysis focused on developing cost-effective energy systems that integrate operating and investment costs, based on high photovoltaic (PV) penetration, using the direct current optimal power flow (DC-OPF) model derived from a linearized network. The results showed that optimizing BESS led to a reduction of 2.28% and 3.38% in PV penetration as well as unsupplied energy costs, respectively compared to scenarios without BESS. Additionally, 25% PV penetration reduced total daily operating costs from fresh battery and SLB by approximately 38.89% and 74.77%, respectively.

Keywords: Battery Energy Storage System; Sizing and Siting; Second-Life Battery; Electric Vehicle Battery; DC-OPF; High Photovoltaic Penetration

1. Introduction

Renewable energy sources (RES) and battery energy storage systems (BESS) are potential solutions to global warming problems by reducing greenhouse gas emissions and promoting a sustainable future[1,2),3)]. Among several RES alternatives, photovoltaic (PV) offers direct integration in power systems, facilitating easy implementation across various regions, including in rural areas. However, the production of PV is severely affected by solar irradiation and ambient temperature[4),5–8)]. Penetration of high-frequency renewable energy plants also affects network stability due to reverse current flow, as well as voltage, frequency, and harmonic[9,10),11)]. To address these challenges, the government has taken measures to significantly increase penetration of renewable energy into local and regional distribution network, focusing on improving the reliability of infrastructure[12–14)]. As a potential solution, BESS offers improved energy efficiency and network stability, ensuring high penetration of renewable energy[15–17)]. Furthermore, it can provide flexibility by storing excess electricity and reducing power supply during peak hours of RES to increase the number of connected RES power sources to the network[18)]. This makes optimization essential to increasing network flexibility, minimizing installation and operation costs[19,20)]. By supporting a high penetration of RES, BESS is capable of preventing load loss and reducing the cost of adding a generator unit to system for backup power[21)]. Additionally, it can reduce the need for additional investment in transmission and distribution infrastructure, along with energy storage and distribution costs.

BESS offers promising solutions for energy supply volatility, with several benefits, including backup, load conversion, auxiliary services, peak shaving, microgrid, integrated renewable energy, frequency regulation, demand response, load leveling, voltage control, and seasonal storage[22),23,24)]. Despite the potential of mitigating power fluctuations and improving grid system performance, there is a significant challenge in determining the appropriate capacity and locations of installed BESS. The lack of capacity and inappropriate locations can lead to significant power losses, higher investment, and operational costs for microgrid systems [25,26),27)]. Consequently, careful consideration and precise determination of capacity and location are essential to achieve optimal performance and economic sustainability. Effective use of BESS can maximize effectiveness and improve the performance of grid systems, contributing to the successful integration of renewable energy into local and regional public network.

Investment costs are directly proportional to the size of BESS, including energy and power ratings, installation, and annual maintenance costs. Although a large capacity of BESS is not economically feasible, an insufficient ability can lead to unrealized benefits [28)]. The cost of BESS is determined by several factors, such as battery technology, energy source integration, location, installation, maintenance, converter interface energy, and capital costs for storage capacity. Other factors include battery life, capacity, degradation, power loss, state of charge (SOC), and depth of discharge (DOD)[11,29,30)]. This phenomenon shows the need for determining the cost-effectiveness of BESS to evaluate the appropriate capacity and installation location for enhancing the performance of grid systems.

Optimal BESS capacity and installation location are crucial to improve the performance and sustainability of the electric system and reduce costs[31),19)]. The optimization process considers several factors such as capacity, locations, and impact on energy losses, along with investment and operating costs. The size of BESS must be balanced with energy cost and rating, including installation and maintenance[27),28)]. Consequently, the optimization process should ensure the economic and sustainable functioning of the electricity system. Improving BESS location in the grid systems is essential for effective response to changes in electricity production and demand. This improvement will reduce losses due to transmission and distribution, thereby removing restrictions on renewable energy production[32)].

Addressing environmental concerns is crucial when dealing with waste from used batteries. Recycling and reusing damaged batteries offer promising solutions. The lead acid battery has a recycling rate of 95% or higher[19,33)], while lithium-ion (Li-ion) is the preferred option for electric vehicle (EV), due to its efficiency[34)]. In the past decade, approximately 400 GWh of Li-ion battery has been sold from 5 million EV worldwide[35)]. However, battery recycling and reusing are complementary processes that reduce the production of unnecessary resources, leading to a significant supply of second-life battery (SLB), as EV market develops.

A recent study suggested that recycling Li-ion battery is not financially viable[36)], showing the need for innovative solutions including repurposing EV SLB as a BESS. However, the reuse of end-of-life battery (EOL) for the construction of BESS can address disposal problems and provide various electrical system services[37)]. Battery that even reached EOL can still be used for lower-demand grid services[38)]. Additionally, the use of SLB has increased the RES capacity of reverse-rotating energy systems and reduced the installation cost [39,40)].

Previous studies have used various methods for optimizing BESS such as evolution algorithms (EA)[37)], rule-based (RB)[41)], model predictive control (MPC)[42)], moving average (MA)[43)], ramp rate controller, mixed integer linear programming (MILP) [44,45)], and mixed

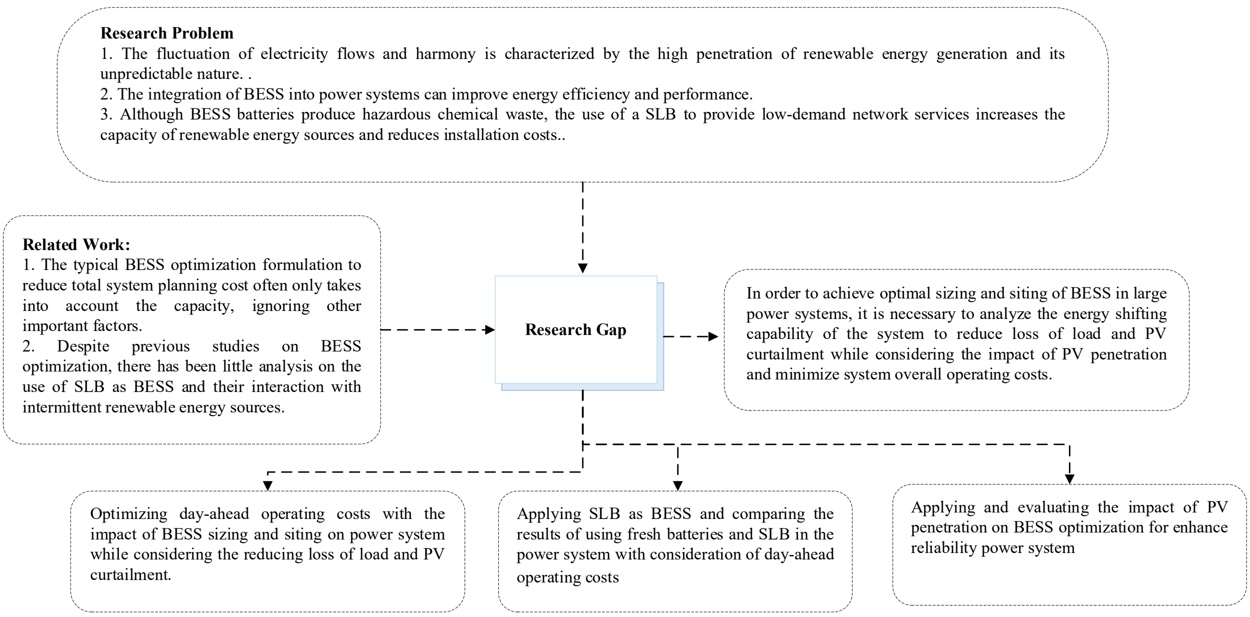

Fig. 1: Overview of study gap BESS

integer nonlinear programming (MINLP) [46]. Typically, optimization methods for power systems depend on nonlinear models, leading to computational challenges. To address these challenges, several power system methods have been developed using MILP to reduce computational load and enable the integration of more generators as well as RES. Additionally, various analysis tools have been used in power system models such as economic dispatch (ED), alternating current optimal power flow (AC-OPF), direct current (DC)-OPF, and unit commitment (UC). These models serve as essential frameworks for understanding and optimizing power system operations.

After conducting a review of previous studies presented in Table 1, certain knowledge gaps have been identified as follows:

- Studies [41,42,46,47] have evaluated the integration of PV and BESS into power systems, without considering the impact of penetration, leading to network instability, overcapacity, and economic losses. Therefore, there is a need to consider the effects of PV penetration for an accurate assessment of feasible and sustainable integration.

Table 1. Literature review of optimizing BESS

Ref.	PV	Wind	Level Penetration VRE	BESS					Power System Model				Model Algorithm
				Fixed Size and Siting	Optimal Sizing	Optimal Siting	Fresh Battery	Second Life Battery	ED	AC-OPF	DC-OPF	UC	
37)					✓			✓	✓				EA
42)	✓			✓			✓			✓			MPC
41)	✓				✓		✓		✓				RB
47)	✓				✓		✓		✓				N/A
46)	✓				✓		✓		✓				MINLP
48)	✓	✓			✓		✓					✓	MILP
45)	✓				✓		✓				✓		MILP
50)		✓	✓	✓	✓		✓				✓		MILP
52)		✓			✓	✓	✓				✓		MILP
43)	✓				✓			✓	✓				MA Ramp Rate Controller
64)	✓			✓				✓	✓				N/A
65)	✓				✓			✓	✓				N/A
66)	✓	✓		✓			✓	✓	✓				N/A
44)	✓	✓	✓	✓			✓					✓	MILP
This Paper	✓		✓	✓	✓	✓	✓	✓			✓		**MILP**

- Previous studies [45,48–51] have examined the impact of energy storage size on the reliability of power systems. However, the majority of studies predominantly focused on sizing, without considering the significance of BESS locations or assessing SLB as an alternative.
- Although previous studies [45,48,52] have addressed the optimization of operation costs and planning for integrated power systems that incorporate BESS and RES, the analysis only considers the cost of load loss. This phenomenon leads to an incomplete assessment of the feasibility and sustainability of integrated systems. Therefore, incorporating penalty costs for RES curtailment is essential to ensure an accurate assessment of a feasible and sustainable power system.

The integration of SLB into BESS presents a significant challenge due to limited capacity. However, the process can still be effective in less demanding network services and increase the renewable energy capacity of reverse spinning applications. In this study, the proposed BESS optimization model aims to address the limited capacity of SLB and compare efficiency with fresh battery. Furthermore, this model considers cost reduction and load loss of PV to reduce operating costs and improve system reliability. Based on these factors, the model is designed to optimize the size and location of BESS to develop cost-effective energy systems that combine operating and investment costs, considering the impact of SLB and PV penetration. The proposed model uses MILP to determine optimal size and location of the BESS grid scale to determine optimal configuration and location of the grid scale.

The study aims to fill the knowledge gaps by proposing a daily optimization method to improve the electricity system through the integration of BESS and PV sources. To address these gaps, the study provides a perspective on the feasibility and sustainability of SLB and PV integration into electricity systems, showing the potential for cost-effectiveness and reliability improvements. For these limitations, the analysis focuses on optimizing BESS size and location only by comparing the results of fresh battery with the Li-ion technology and the SLB. The optimization of energy systems is conducted using the DC-OPF model, which is developed from a linearized network model.

The main contributions to this study are summarized as follows.

- The study presents a formula considering the effect of the size and location of the BESS on the electricity system when calculating daily operational costs. Furthermore, the proposed model considers the potential impact of load loss and PV curtailment, capable of affecting daily operating costs.
- The application of Li-ion battery as BESS is assessed and compared with results to those obtained from the use of fresh battery in power systems. A comparison is carried out to determine the impact of daily operating costs on the performance of two batteries.
- The study evaluates the impact of PV penetration on the optimization of BESS in the electrical system.

The structure of the study is as follows: Section 2 describes the mathematical models used to optimize BESS. Section 3 explains how to determine optimal BESS sizes and position strategies, while Section 4 describes the case studies. Meanwhile, section 5 evaluates and discusses the results of the optimization. Discussion continued in Section 6 and presented the conclusions, while further work was presented in Section 7.

2. Problem Formulation

The optimization of sizing and siting of BESS is essential to develop cost-effective power systems that balance operating and investment costs. The process is carried out to improve reliability and durability[53)], thereby reducing total losses and costs. To achieve this, BESS optimal positioning depends on the size results of each grid location. Based on investor objectives, size strategies are formulated to determine optimal BESS capacity of the network considering battery energy capacity (MWh) and power rating (MW), along with technology and characteristics. Previous studies have shown that optimal siting of BESS improves the response to changes in electricity production and demand[50,53)]. Therefore, the day-ahead optimization for power systems with integrated BESS and PV functions is formulated as follows:

$$Min\,TOC = C^{g} + C^{pvc} + C^{ens} + C^{bess} \quad (1)$$

$$C^{g} = \sum_{i,,t,g}\left(a_g\left(P_{g,t}^{G}\right)^2 + b_g\left(P_{g,t}^{G}\right) + c_g\right) \quad (2)$$

$$C^{pvc} = \sum_{i,t}\mu_i^{pvc}P_{i,,t}^{pvc} \quad (3)$$

$$C^{ens} = \sum_{i,d,t}\mu_i^{VOLL}P_{i,t}^{LS} \quad (4)$$

$$C^{bess} = \frac{\sum_{b,i}P_{b,i}^{BESS}\left(\mu_b^{Ep}+\mu_b^{Eom}\right)+E_{b,i}^{BESS}\left(\mu_b^{Ee}+\mu_b^{Eins}\right)}{365\,T_b^{Lt}} \quad (5)$$

The daily total operating cost (TOC) connected to the grid is shown in Eq (1), including generators, operating costs (C^{g}), BESS cost (C^{bess}), energy does not supply cost (C^{ens}), and PV curtailment cost (C^{pvc}). The indices used in Eq (2-5) are g for the generator unit, i,j for the bus unit, battery technology type with b, and the period index in hours with t. The coefficients a_g, b_g, c_g represent the fuel cost of generators, $P_{g,t}^{G}$ is the generator output power in MW, μ_i^{pvc} represent the penalty cost of PV curtailment, and $P_{i,t}^{pvc}$ is PV curtailment power in MW.

In Eq. (4) represents the value of lost load (VOLL) and the load shedding power. μ_i^{VOLL} represent the value of penalty VOLL and, $P_{i,t}^{LS}$ represent the load-shedding power in MW. VOLL is calculated to estimate the monetary losses caused by unused energy resources. The price is determined by the willingness of customers to pay for reliable electricity services, depending on the location, type of customer, and periods of the power outage[54)].

The cost of installation and operation are shown in Eq. (5), where $P_{b,i}^{BESS}$ represents the BESS power capacity in MW, $E_{b,i}^{BESS}$ is BESS energy in MWh, and μ_b^{Ep} is the investment cost per capital capacity power rating. Additionally, μ_b^{Eom} represents BESS operation and maintenance costs, μ_b^{Ee} is the capital energy rating of the investment costs, and μ_b^{Eins} as BESS installation costs. In this objective function, the cost of BESS is divided by 365 days, with T_b^{Lt} representing the service lifetime of battery in years or EOL.

2.1 Grid Balance Operation Constraint

$$\sum_{g,t}P_{g,t}^{G} + \sum_{b,t}\left(-P_{b,t}^{ch} + P_{b,t}^{dch}\right) + P_{i,t}^{pv} + P_{i,t}^{LS} - P_{i,t}^{LD} = P_{i,j,t} \quad (7)$$

$$P_{i,j,t} = \frac{\delta_{i,t}-\delta_{j,t}}{X_{i,j}} \quad (8)$$

$$-P_{i,j,t}^{max} \leq P_{i,j,t} \leq P_{i,j,t}^{max} \quad (9)$$

$$0 \leq P_{i,t}^{LS} \leq \left(P_{i,t}^{LD}\right) \quad (10)$$

A constraint is introduced in Eq. (7) to ensure the balance of energy and power in system. This constraint requires that power generated by generators and PV systems located on bus flowing to and fro is equivalent to the local demand. When the output is not sufficient to meet the balance, a load shift occurs, where Ih corresponds to power flow of the bus in relation to the branch network. The discharge power of BESS is denoted as $P_{b.t}^{dch}$ in MW, while $P_{b.t}^{ch}$ is charging power. The positive value of the BESS represents the discharge, while the negative value shows charge. The active power output from PV is denoted as $P_{i,t}^{pv}$ and the active power of the load is $P_{i,t}^{LD}$. Moreover, Eq. 8 represents the active current flow of the branch connected to the bus, which corresponds to the voltage angle between the bus and the reaction voltage $P_{i,j,t}$. The voltage angle i, is denoted as $\delta_{i,t}$ and the reactance branch is $X_{i,j}$. In Eq. 9, the maximum power flow limits for bus connected to branches are defined as $P_{i,j,t}^{max}$, thereby power flow of the bus connection branch is restricted. Finally, Eq. 10 defines the limit of load loss power.

2.2 Generator Operation Constraint

$$P_{g,t}^{G,min} \leq P_{g,t}^{G} \leq P_{g,t}^{G,max} \quad (11)$$

$$P_{g,t}^{G} - P_{g,(t-1)}^{G} \leq RU_g \quad (12)$$

$$P_{g,(t-1)}^{G} - P_{gt}^{G} \leq RD_g \quad (13)$$

When the generator functions within the operating limits, power supply capacity of the grid is limited by Eq. (11). This process considers the minimum and maximum limit for the generator power output, represented by $P_{g,t}^{G,min}$, and $P_{g,t}^{G,max}$respectively. Equations (12) and (13) represent the limits for ramping up (RU_g) and ramping down (RD_g) the output power of generators, respectively.

2.3 PV Operation and Curtailment Constraint

$$0 \leq P_{i,t}^{pv} \leq pv_{i,t}\Lambda_i^{pv} \quad (14)$$

$$P_{i,t}^{pvc} = pv_{i,t}\, \Lambda_i^{pv} - P_{i,t}^{pv} \quad (15)$$

Eq. (14) describes the availability power PV constraint that includes power of bus-connected PV $pv_{i,t}$, with Λ_i^{pv} representing PV capacity in MW. Meanwhile, Eq. (15) is the value power PV available at less than the active output.

2.4 BESS Operation Constraint

$$0 \leq P_{b.i.t}^{dch} \leq P_{b,i}^{BESS} \quad (16)$$

$$-P_{b,i}^{BESS} \leq P_{b,i,t}^{ch} \leq 0 \quad (17)$$

$$SOC_{b,i,t}^{BESS} = \left(1-k_b^{sd}\right) SOC_{b,i,(t-1)}^{BESS} + \left(\eta_b^{ch} P_{b,i,t}^{ch} + \frac{P_{b.i.t}^{dch}}{\eta_b^{dch}}\right) \quad (18)$$

$$0 \leq SOC_{b,i,t}^{BESS} \leq E_{b,i}^{BESS} \quad (19)$$

Eq. (16) defines the maximum power that BESS can discharge at any given time. Similarly, Eq. (17) represents the limit on BESS power rating when charging. In Eq. (18), the SOC $SOC_{b,i,t}^{BESS}$ is constrained by the balance of its energy capacity, considering self-discharge of battery k_b^{sd}, as well as the efficiency of BESS during charging η_b^{ch} and discharge η_b^{dch}. The continuity of energy stored is expressed in Eq. (19) based on consistent BESS, except for changes caused by charges and discharges. This equation ensures consistent energy stored at the end and beginning of the next interval, considering energy added or extracted during the process.

3. Proposed Methodology

The main objective of BESS sizing and siting optimization is to determine optimal value of power rate variable $P_{b,i}^{BESS}$ and energy rate $E_{b,i}^{BESS}$, to minimize daily total operation costs. This optimization is performed using Optimal Power Flow (OPF), based on operating model constraints of the electrical system, to improve distribution, and reduce the fuel costs of the electrical plant. To evaluate the effect of the BESS on the daily operating costs, PV curtailment, energy loss, and the BESS were added to the objective function Eq. (1). Several BESS optimization algorithms are based on Mixed-Integer Nonlinear Programming (MINLP) and Mixed-Integer Linear Programming (MILP)[55]. However, the complexity and nonlinearity of MINLP is larger than the proposed model, requiring time and computational resources, to target the most favorable local solution[53]. MILP algorithm is relatively simple, inexpensive, and capable of accommodating a large number of RES and loads. It also handles numerous constraints, showing a low amount of forecasting error.

In this study, the network model uses a DC-OPF, which is linearized to mitigate computational complexity from the "curse of dimensionality". DC-OPF model is introduced to simplify power flow equations and mitigate the computational complexity associated with the AC-OPF problem using a quadratic function to represent bus angles and losses. However, as system reaches stress conditions, the active power transfer is often limited by voltage and reactive power constraints. This shows the need to integrate voltage/VAR constraints into OPF model. Various efforts have been made to incorporate Q and v into linearized network models. To address the nonconvexity introduced by quadratic losses, an enhanced linearized network model based on Taylor series expansion is applied to OPF problem. Additionally, a method using piecewise linearization with integer variables is proposed to manage the nonconvex nature of quadratic losses[56].

MILP algorithm using a branch and bound strategy is applied to optimize the problem. The bound process aims to determine a solution to the relaxed problem, serving as

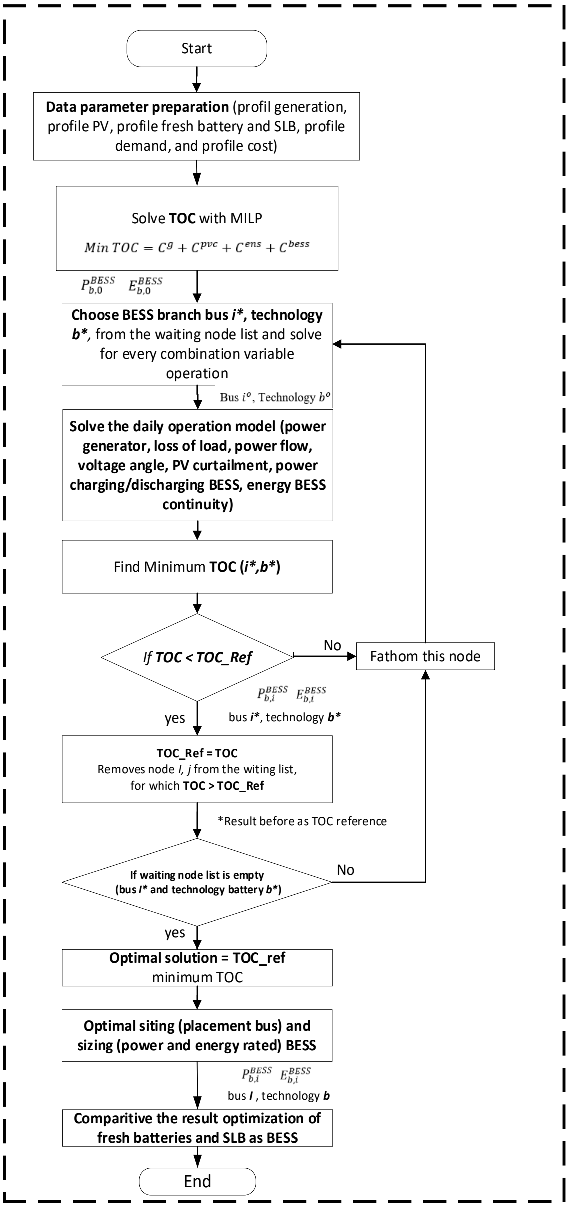

Fig. 2: Flowchart optimal siting and sizing BESS

a lower limit for minimization or a higher limit for maximization. Meanwhile, the branch process entails dividing the problem into smaller parts. The branch and bound strategy consists of two critical steps, namely fathomed and incumbent nodes. Specifically, fathomed nodes do not require re-branching, as MILP is impossible, suggesting that a feasible or optimal solution has been found. Incumbent nodes represent the best solutions at each search node. For example, when an integer solution is performed with a better objective function value or there are no incumbent nodes at the start of the search, the recent solution becomes the new incumbent node.

4. Case Studies

The test network used for evaluation was the adapted IEEE 14 test bus system. Generators were placed on buses 1 and 3, while bus 4 was equipped with PV power sources. Tables A1, A2, and A3 show resistance, reaction, generators, bus system data, and daily load data[57,58]. Diagram IEEE-14 modified is shown in Figure 3. The load profile is shown in Figure 4[59] and in Figure 5 shows hourly PV profile data obtained from the National Renewable Energy Laboratory (NREL)[60].

Table 2. Data parameter fresh battery and SLB [35,52,53,61,62]

Parameter	Fresh Battery	SLB
Efficiency (%)	95	90
Self-Discharge on Daily (%)	0.02	0.1
Cost of BESS Power Rate ($/kW)	320	320
Cost of BESS Energy Rate ($/kWh)	360	80
Installation Cost ($/kWh)	15	37
Cost of Maintenance System ($/kW/Year)	5	7.78
Lifetime (Years)	10	6

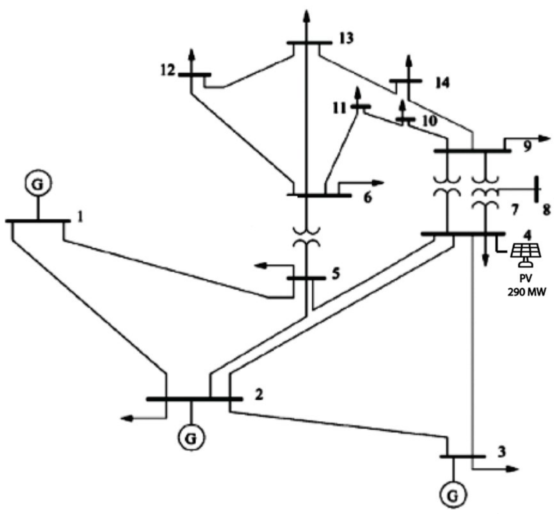

Fig. 3: Diagram IEEE-14 modified [57,58]

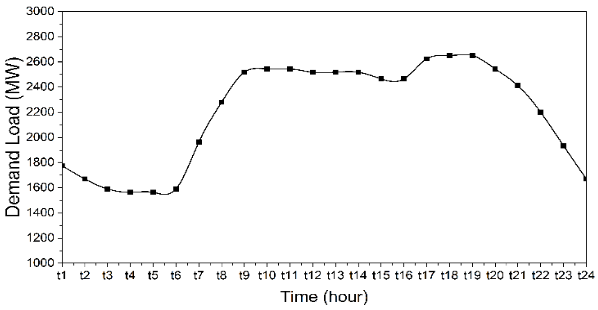

Fig. 4: The data on the hours of load demand for the modified IEEE-14 bus

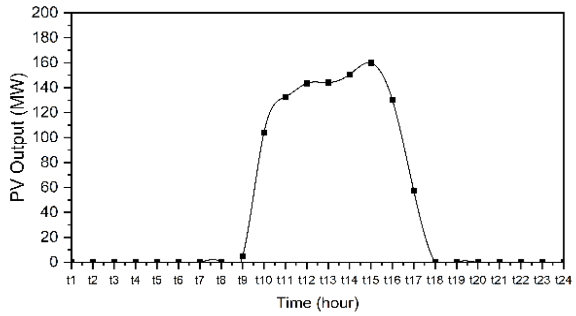

Fig. 5: Hourly PV data for modified IEEE-14 bus

Table 3. PV penetration scenario

Scenario	PV Penetration	Location PV on Bus
1	10 %	4
2	25 %	4,6
3	50 %	4,6,11,14
4	100 %	4,5,6,8,10,11,12,14

This study uses two types of Li-ion battery, consisting of fresh and SLB from EV, as shown in Table 2[35,53,61], with a service time (T_b^{Lt}) of 10 years[52], and 6 years, respectively[62]. In this study, both fresh battery and SLB share the same criteria, while the investment cost is normalized to one day. Figure 2 shows the PV penetration scenario in the bus system. Table 3 shows the scenario PV penetration. Furthermore, the proposed MILP model was implemented in general algebraic modeling system (GAMS) 39.2.1 and calculated using AMD Ryzen 5 3550h 3.6GHz CPLEX LP solver with 16GB RAM.

5. Numerical Result

The study examines the impact of the use of fresh batteries and SLB on energy system costs in BESS To achieve this objective, five different scenarios were analyzed, each including a new PV penetration scenario:

Case A: Represents the daily operation of the electrical system without BESS.

Case B: The use of fresh battery with a fixed size and location of BESS.

Case C: The use of SLBs and the fixed size and location of BESS is considered.

Case D: Examines the use of a fresh battery with optimized BESS size and site.

Case E: Evaluate the use of SLBs with optimized BESS size and site

Case A was selected as a basis for establishing benchmark to assess the effectiveness of BESS system. Meanwhile, Cases B and C were designed to compare the impact of fixed power supply and location on BESS, fresh battery, and SLB. Cases D and E were used to determine optimal capacity and location.

In case A, there was no BESS on power system and the optimization problem was used to minimize the network operating costs. These included the cost of producing generators, unsupplied energy, and PV curtailment. The penalty fee for the load shedding, PV curtailment penalty, and total daily operating costs used were $/MWh 50,000 [53], 50 $/MWh [63] and $8,779,631, respectively.

Simulation results showed that there was a significant difference between load demand and electricity production by generators in the 3rd to 16th hours, leading to load losses, as shown in Fig.6. The study found that in the case of 10% PV penetration, the most economical reduction fee was $14,668.71. This occurred when PV energy production could not be reduced to meet load demand and distributed power generation. However, when PV penetration rate was 100%, a significant reduction was observed in the TOC. These results showed that increasing the PV penetration rate could be a cost-effective solution to reducing network operating costs.

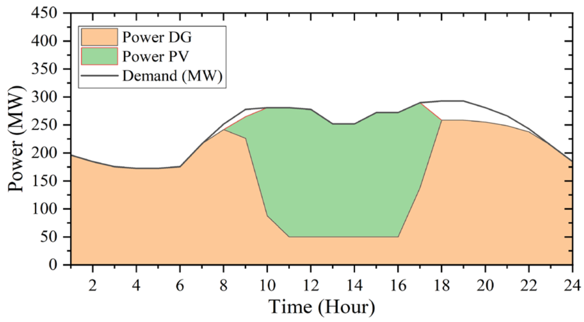

Fig. 6: The dispatch of power system in case A PV penetration 100%

Table 4. The results of numerical simulation on case A

PV Penetration	10%	25%	50%	100%
C^g ($)	13,933.72	12,110.59	11,492.22	11,416.99
C^{ens}($)	8,684,134.65	7,420,858.31	7,246,366.98	6,993,096.99
C^{pvc}($)	14,668.71	28,942.29	122,235.39	326,209.54
C^{bess}($)	-	-	-	-
TOC($)	8,712,737.09	7,461,911.20	7,380,094.60	7,330,723.53

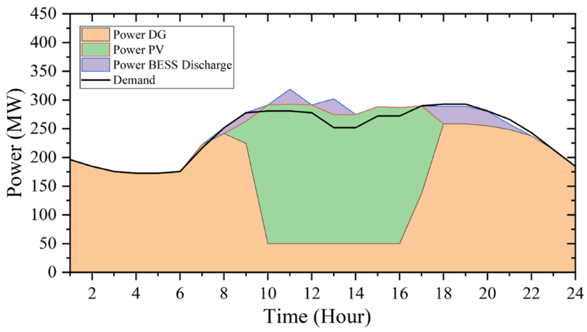

Fig. 7: The dispatch of power system in case B PV penetration 100%

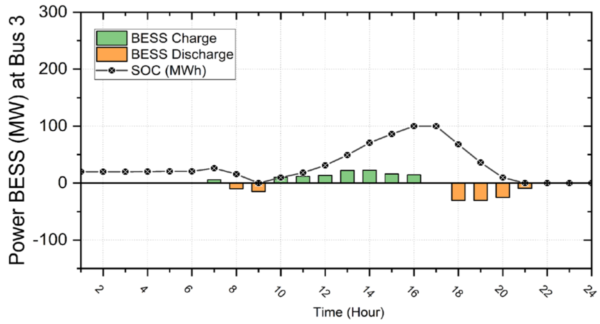

Fig. 8: The hourly dispatch of BESS on Case B PV penetration 100%

Table 5. The results of numerical simulation on case B

PV Penetration	10%	25%	50%	100%
C^g (\$)	14,669.32	12,567.51	11,546.56	11,378.96
C^{ens}(\$)	2,181,432.83	1,130,326.78	1,089,802.07	1,089,802.07
C^{pvc}(\$)	19,176.34	28,573.62	115,868.10	318,763.33
C^{bess}(\$)	147,2602.74	1,472,602.74	1,472,602.74	1,472,602.74
TOC(\$)	3,687,881.23	2,644,070.65	2,689,819.48	289,2547.11

Case B was selected to minimize load losses and reduce PV energy by implementing BESS. Initially, the fixed sizing and siting values of BESS variables, $P_{b,i}^{BESS}$ and $E_{b,i}^{BESS}$ in Eq. 5, were used to determine optimal solution. Simulation was carried out to evaluate the daily operation of power system without considering the replacement cost. This experiment was carried out to investigate the effects of using fresh Li-ion battery in power systems, considering the operation limitations of BESS, as specified in Eq. (16-19). However, the maximum DOD strategy was not considered in the optimization phase and the maximum value was set to 80%. BESS with a capacity of 100 MWh energy and 50 MW power was installed at bus 3. This siting was strategic due to the proximity to both demand centers and power generation facilities.

Based on the simulation results, the use of fresh Li-ion battery in energy systems effectively reduced energy costs and PV excesses. BESS showed the potential capacity to discharge energy and meet demand when energy generated is not enough. In a 100% PV penetration scenario, BESS reduced unsupplied energy costs that were not supplied by 3.38% and PV curtailment by 2.28% compared to case A. As shown in Fig. 8, hourly delivery of BESS followed the two charge-and-discharge cycles of the day, supporting energy demand in the event of load loss during the 7th and 17th hours. These results suggested that the implementation of BESS with a fixed size and siting value could improve energy system, although with impact limited by the fixed capacity of battery.

In this study, operating costs were obtained from generators, unsupplied energy, PV curtailment, and BESS operation. The simulation results presented in Table 5 showed that the TOC was lower in the 25% PV penetration scenario. Although BESS did not fully compensate for load loss, it minimized load losses and PV curtailment by providing electricity reserves. BESS also significantly reduced TOC by 64.5%, showing potential as an economically efficient solution to reduce operating costs and improve the reliability of high-power PV penetration systems.

In case C, the use of SLB was examined rather than BESS. The SLB was installed on bus 3 with power capacity of 100 MWh and energy rate of 50 MW. This placement was strategic due to proximity to both demand centers and power generation facilities. The SLB was connected to two charging and discharge cycles daily, as shown in Fig. 9 and 10. The results in Table 6 showed that the TOC of 25% of PV penetration scenarios were lower than Case B. SLB and BESS were used to reduce operating costs by 68.64% compared to Case B, resulting in total daily operating costs of \$1,887,635.54.

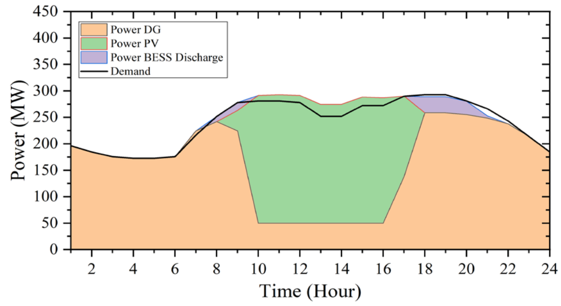

Fig. 9: The dispatch of power system in case C PV Penetration 100%

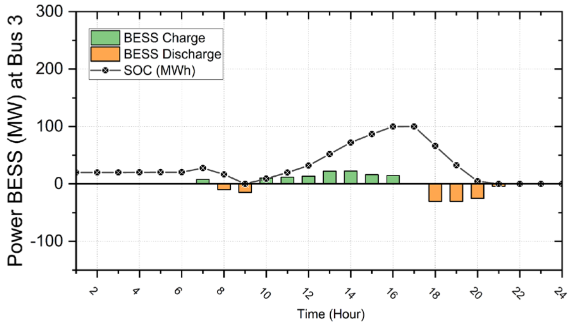

Fig. 10: The hourly dispatch of BESS on case C PV penetration 100%

Table 6. The results of numerical simulation on case C

PV Penetration	10%	25%	50%	100%
C^g (\$)	14,649.46	12,608.12	11,580.25	11,387.59
C^{ens}(\$)	2,470,324.74	1,384,716.81	1,342,769.41	1,342,769.41
C^{pvc}(\$)	18,116.38	28,573.62	115,868.10	318,763.33
C^{bess}(\$)	461,736.98	461,736.98	461,736.98	461,736.98
TOC(\$)	2,964,827.58	1,887,635.54	1,931,954.75	2,134,657.33

Case D focused on optimizing BESS size and location to determine the impact on total power system operating costs. Initially, the variables $P_{b,i}^{BESS}$ and $E_{b,i}^{BESS}$ were used to determine optimal configuration that would lead to the minimum daily operating costs. Table 7 shows that BESS is optimally configured in buses 3, 9, and 11, while the total capacity with 25% PV penetration is 34.05MW and 123.73MWh. Figures 11 and 12 show that the optimized BESS experiences two charge/discharge cycles per day. By optimizing the size and location of the BESS, there is the possibility to minimize the cost of energy generation and PV production. Based on the results, the cost of BESS is lower than the 50% and 100% PV penetration scenarios. However, optimization of BESS configuration led to the reduction of TOC by 38.89% compared to case B. This showed the potential advantages of optimizing the size and location of BESS for high PV penetration.

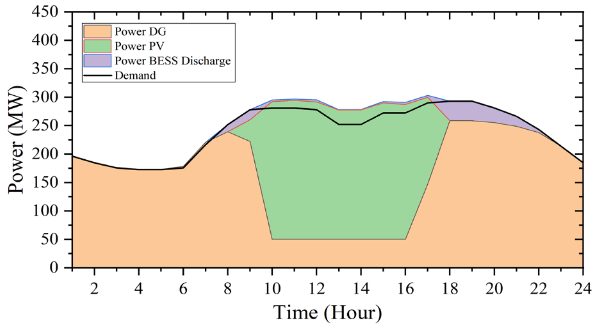

Fig. 11: The dispatch of power system in case D PV penetration 100%

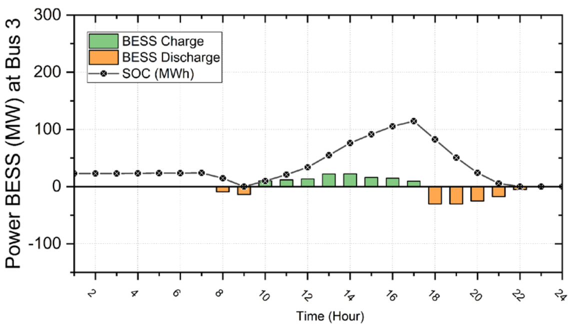

Fig. 12: The hourly dispatch of BESS on case D PV penetration 100%

Table 7. The results of numerical simulation on case D

PV Penetration	10%	25%	50%	100%
C^g ($)	147,92.00	12,633.18	11,572.95	11,394.26
C^{ens}($)	-	-	-	-
C^{pvc}($)	189,77.28	28,495.58	115,203.50	318,216.47
C^{bess}($)	1,765,310.78	1,574,565.64	1,566,504.17	1,56,6504.17
TOC($)	1,799,080.06	1,615,694.42	1,693,280.63	1,896,114.91

Table 8. The results of optimizing BESS on case D

PV Penetration	Bus Location Placement of BESS	Power Rating (MW)	Energy Rating (MWh)
10%	3	30.18	125.88
	8	0.88	1.86
	9	3.90	13.7
25%	3	30.32	115.19
	9	3.48	8.01
	11	0.25	0.53
50%	3	30.32	114.40
	9	2.91	6.80
	10	0.82	1.73
100%	3	30.32	114.40
	9	2.91	6.80
	10	0.82	1.73

In case E, SLB was designed to optimize size and location using BESS to minimize daily operating costs. The optimization used variables to determine optimal configuration. The results in Table 9 dan 10 showed that buses 3, 9, and 11 had optimized SLB configuration with a total capacity of 34.05MW and 130.740MWh under the 25% PV penetration scenario. Figures 13 and 14 show that optimized SLB had two charging/discharge cycles/day. This optimization using SLB resulted in a cost reduction of 74.77% in Case C in the same scenario. The implementation of SLB instead of BESS significantly reduced the operating costs of power systems, while meeting the same performance requirements.

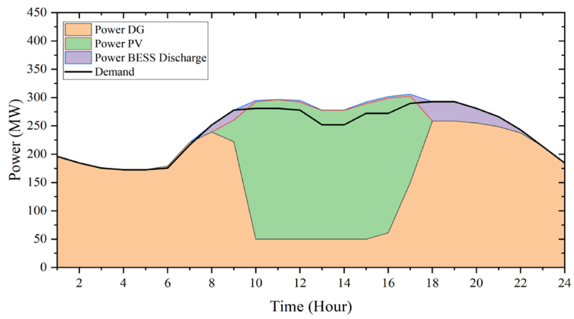

Fig. 13: The dispatch of power system in case E PV Penetration 100%

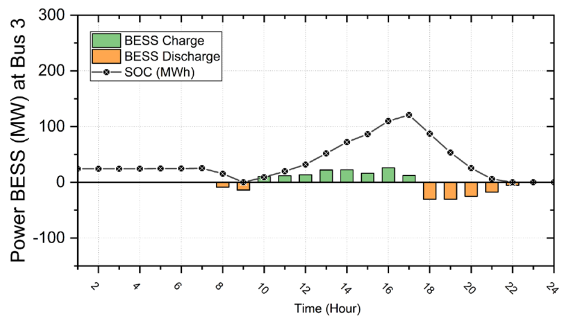

Fig. 14: The hourly dispatch of BESS on case E PV penetration 100%

Table 9. The results of numerical simulation on case E

PV Penetration	10%	25%	50%	100%
C^g (\$)	14,809.64	12,700.91	11,633.80	11,451.60
C^{ens}(\$)	-	-	-	-
C^{pvc}(\$)	17,919.92	28,475.95	115,086.85	318,078.64
C^{bess}(\$)	477,342.08	435,026.32	4,33,352.25	4,33,352.25
TOC(\$)	510,071.65	476,203.19	560,072.90	762,882.50

Table 10. The Results of Optimizing BESS on case E

PV Penetration	Bus Location Placement of BESS	Power Rating (MW)	Energy Rating (MWh)
10%	3	30.16	132.99
	7	0.80	1.79
	8	0.05	0.12
	9	3.92	15.36
25%	3	30.32	121.72
	9	3.48	8.46
	11	0.25	0.56
50%	3	30.32	120.85
	9	2.91	7.18
	10	0.82	1.83
100%	3	30.32	120.85
	9	2.91	7.18
	10	0.82	1.83

The optimization of energy systems is essential to ensure efficient and sustainable energy production. Therefore, this study focused on identifying the main challenges of system optimization and determining solutions using BESS.

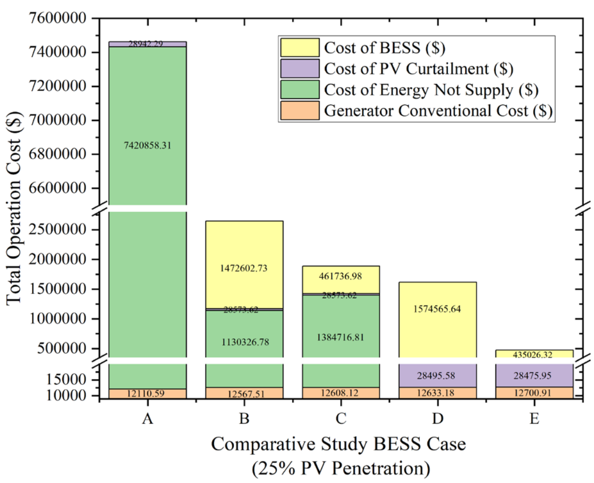

Fig. 15: Comparative study total operation cost

Table 11. Comparative study BESS

Case 25% PV Penetration	Objective Function (\$/day)	Optimal Location BESS (bus)	Total Power BESS (MW)	Total Energy BESS (MWh)
A	7,461,911.20	-	-	-
B	2,644,070.65	3	50	100
C	1,887,635.54	3	50	100
D	1,615,694.42	3, 9. 11	34.05	123.73
E	476,203.19	3, 9. 11	34.05	130.74

Analysis of five case scenarios showed that energy costs, supply, and PV curtailment were the main issues of system optimization. Case A showed that power imbalance could lead to a high energy cost, significantly resulting in load loss. However, simulation results showed that BESS supported high PV penetration, prevented peak-hour production, improved reliability, and reduced load loss.

In case A, BESS avoids investment costs but results in high energy consumption. Meanwhile, in cases B and C, the addition of BESS led to a reduction in losses and TOC. Table 11 shows that the daily operating costs of using SLB as BESS are the lowest, showing the size and location of Case E as optimal. The use of the same capacity and location also reduced the operating costs of BESS compared to fresh battery.

The results showed that SLB was more economical than fresh battery mainly due to lower energy costs. In cases D and E, installation sites close to load plants, solar power plants, and generators were identified as optimal locations for BESS. This result was directly influenced by the constraint grid balance in Eq (7), where BESS selected optimal location within the installation bus to handle the excess load demand caused by electric energy generation. In cases A to C, high PV penetration into system increased the cost associated with PV curtailment. However, TOC were reduced due to lower energy and load. In cases D and E, optimizing energy conversion by BESS and charging was reversed to recover load loss costs and PV compression.

The optimization process showed that the TOC objective function of cases B and D was high in BESS. These results were obtained from optimal size and location of BESS, showing the daily number of charge/discharge cycles, as presented in Fig. 8, 10, 12, and 14. The study found that optimal BESS usually only passed two cycles on average daily. Excessive cycles had a negative impact on the lifespan of BESS, particularly for long-term system applications.

The results showed that the implementation of optimal BESS system could reduce load loss in energy system and the costs of PV generation. The operating cost of optimal BESS was reduced from 38.89% to 74.77% for fresh battery and SLB without optimization. However, the reliability of the service life must be considered as SLB and fresh battery only lasts for 6 years and 10 years, respectively.

This study showed the importance of SLB in addressing battery disposal issues and improving the capacity of RES by enhancing system's ability to handle reverse energy flow. By optimizing BESS sizes and locations using fresh battery and SLBs, a significant reduction in energy costs was achieved. In comparison, optimally configured BESS minimized PV curtailment and energy supply costs. Additionally, daily operating costs were reduced, despite the shorter lifespan of the SLB. This suggested that optimal BESS installation reduced energy costs, leading to improved system reliability and effective management of PV penetration levels. Optimal BESS charge and discharge schedule also enabled the load transfer system to operate efficiently.

7. Conclusion

In conclusion, this study showed that the integration of renewable energy into the electricity grid caused various challenges such as voltage and frequency fluctuations, harmony, and reverse energy supply. To address these challenges, BESS was identified as a promising solution, to enhance grid stability, energy efficiency, and enable more effective use of renewable energy. This study also emphasized the potential of SLB in addressing battery disposal and mitigating the capacity of RES by improving system's ability to handle reverse energy flow. Therefore, analysis was carried out to optimize the size and location of BESS, using both fresh battery and SLB, to minimize daily operational costs.

The results showed that optimally configured BESS significantly reduced energy costs. This showed that a 25% PV penetration scenario optimized system performance without compromising reliability. Through strategic optimization, BESS showed the potential to lower PV curtailment costs by approximately 2.28% and unsupplied energy costs by 3.38%. Furthermore, optimal sizing and siting of BESS reduced daily operating costs by approximately 38.89% and 74.77% for fresh battery and SLB, respectively. Although initial BESS installation costs increased, total operational costs were substantially reduced, particularly with SLB, which caused a 70.5% reduction. The shorter lifespan of SLB compared to fresh battery posed considerations for long-term investment strategies.

For a more comprehensive understanding of BESS role in grid stability and RES integration, future studies should explore the long-term effects of battery degradation on power system planning and strategies to enhance the UC process. This exploration was recommended to ascertain the full impact of SLB incorporation and RES penetration on the strategic planning as well as operational efficiency of power systems.

Acknowledgments

This research was supported by Universitas Sebelas Maret, Research Grant: Penelitian Disertasi Doktor (PDD-UNS) with contract number 254/UN27.22/PT.01.03/2022.

Conflict of Interest

The authors declare that there is no conflict of interest. Additionally, the study initiatives that were used for support did not play any role in the planning, data collection, analysis, interpretation, composition of the paper, or decision to publish the results.

Author Contributions

Chico Hermanu Brillianto Apribowo contributes to the following phases, concept, methodology, software, data collection, visualization, and writing of original text. Sasongko Pramono Hadi is responsible for conceptualization, data extraction, validation, writing (including review and editing), and supervision. F. Danang Wijaya carries out the design, validation, data collection, writing (review and editing), and supervision. Sarjiya is responsible for ideas, methods, visualization, data collection, validation, writing (revision and editing), supervision, and financing procurement. All authors reviewed the final version of the published work and gave their approval.

Nomenclature

Index

g	Generator unit
i, j	Bus unit
t	Hourly
b	Battery technology

Parameter

a_g, b_g, c_g	Coefficient cost of fuel generator
μ_i^{pvc}	Penalty coefficient for restricted PV units
μ_i^{VOLL}	Penalty coefficient for units to lose load shedding
μ_b^{Ep}	The annual cost of investment/capital of BESS power rating
μ_b^{Eom}	The annual cost of BESS maintenance and operation
μ_b^{Ee}	The annual cost of investment/capital of BESS energy rating
μ_b^{Eins}	BESS installation cost
$P_{i,t}^{pv}$	Active power output from PV

$P_{i,t}^{LD}$	Active power from load demand
$X_{i,j}$	Reactance from bus-connected branches
$P_{i,j,t}^{max}$	Maximum power flow limit from the connected branch bus
$P_{g,t}^{G,min}$, $P_{g,t}^{G,max}$	Minimum limit dan maximum from the generator
RU_g, RD_g	Ramp up dan ramp down
$pv_{i,t}$	Availability of bus-connected PV
Λ_i^{pv}	PV capacity connected to the bus
k_b^{sd}	Coefficient self-discharge battery
η_b^{ch}, η_b^{dch}	Battery charging and discharging efficiency
T_b^{Lt}	Service lifetime manufacture battery

Variable

TOC	Total operating cost
P_{gt}^{G}	Generator output power
$P_{i,t}^{pvc}$	PV curtailment output power
$P_{i,t}^{LS}$	Load shedding power
$P_{b,i}^{BESS}$	Installed BESS power
$E_{b,i}^{BESS}$	Installed BESS energy
$SOC_{b,i,t}^{BESS}$	BESS continuity energy
$P_{b,t}^{ch}$	BESS charging power
$P_{b,t}^{dch}$	BESS discharging power
$P_{i,j,t}$	Active power flow from the connected branch of the bus
$\delta_{j,t}$	Voltage angle of the bus j

Table A1. Generator data for modified IEEE-14 bus

Generator	Bus	Pmax (MW)	Pmin (MW)	RU (MW/h)	RD (MW/h)
G1	1	160	10	80	110
G2	2	80	20	50	65
G3	3	50	20	30	40

Table A2. Cost generator data for modified IEEE-14 bus

Generator	a ($)	b ($)	c ($)
G1	0.005	2.45	105.000
G2	0.005	3.51	44.100
G3	0.005	3.89	40.600

Table A3. Demands of each bus in MW

Bus	Pd	Qd
1	0	0
2	21.7	12.7
3	94.2	19
4	47.8	-3.9
5	7.6	1.6
6	11.2	7.5
7	0	0
8	0	0
9	29.5	16.6
10	9	5.8
11	3.5	1.8
12	6.1	1.6
13	13.5	5.8
14	14.9	5

References

1) C.L. Nguyen, H.H. Lee, and T.W. Chun, "Cost-optimized battery capacity and short-term power dispatch control for wind farm," *IEEE Trans Ind Appl*, **51** (*1*) 595–606 (2015). doi:10.1109/TIA.2014.2330073.
2) T.C. Rudien, T.C. Rudien, D.H. Didane, M.F. Mohideen, K. Abdullah, S. Mohd, B. Manshoor, and S. Al-alimi, "Technical feasibility analysis of wind energy potentials in two sites of east malaysia : santubong and kudat technical feasibility analysis of wind energy potentials in two sites of east malaysia : santubong and kudat," *Evergreen*, **8** (*2*) 271–279 (2021). doi:10.5109/4480703
3) M. Bansal, A. Agarwal, M. Pant, and H. Kumar, "Challenges and opportunities in energy transformation during covid-19 challenges and opportunities in energy transformation during covid-19," *Evergreen*, **8** (*2*) 255–261 (2021). doi:10.5109/4480701
4) E. Nurdiana, V. Nurliyanti, D.A. Rianjani, K. Akhmad, A. Kurniasari, K. Fauziah, Y. Astriani, and S. Syafei, "Performance analysis and comparison of a 93.6 kw grid- connected rooftop photovoltaic system in south tangerang," *Evergreen*, **10** (*3*) 1916–1927 (2023). doi:10.5109/7151746.
5) Y.S. Indartono, A.M. Nur, A. Divanto, and A. Adiyani, "Design and testing of thermosiphon passive cooling system to increase efficiency of floating photovoltaic array," *Evergreen*, **10** (*1*) 480–488 (2023). doi:10.5109/6782151.
6) K. Verma, O. Prakash, A.S. Paikra, and P. Tiwari, "Photovoltaic panel integration using phase change material (pcm): review," *Evergreen*, **10** (*1*) 444–453 (2023). doi:10.5109/6782147.
7) C.H.B. Apribowo, A. Habibie, Z. Arifin, and F. Adriyanto, "Experimental method for improving efficiency on photovoltaic cell with using floating installation method," *AIP Conf Proc*, **2217** (*1*) (2020). doi:10.1063/5.0000827/1025212.
8) M.M. Rahman, S. Saha, M.Z.H. Majumder, T.T. Suki, M.H. Rahman, F. Akter, M.A.S. Haque, and M.K. Hossain, "Energy conservation of smart grid system using voltage reduction technique and its challenges,"

Evergreen, **9** (*4*) 924–938 (2022). doi:10.5109/6622879.

9) S.S. Mendu, P. Appikonda, A.K. Emadabathuni, and N. Koritala, "Techno-economic comparative analysis between grid-connected and stand-alone integrated energy systems for an educational institute," *Evergreen*, **7** (*3*) 382–395 (2020). doi:10.5109/4068616.
10) P. Byrne, N. Putra, T. Maré, N. Abdallah, P. Lalanne, I. Alhamid, P. Estelle, A. Yatim, and A.L. Tiffonnet, "Design of a solar ac system including a pcm storage for sustainable resorts in tropical region," *Evergreen*, **6** (*2*) 143–148 (2019). doi:10.5109/2321009.
11) H. Hao, D. Wu, J. Lian, and T. Yang, "Optimal coordination of building loads and energy storage for power grid and end user services," *IEEE Trans Smart Grid*, **9** (*5*) 4335–4345 (2018). doi:10.1109/TSG.2017.2655083.
12) Y.M. Atwa, and E.F. El-Saadany, "Optimal allocation of ess in distribution systems with a high penetration of wind energy," *IEEE Transactions on Power Systems*, **25** (*4*) 1815–1822 (2010). doi:10.1109/TPWRS.2010.2045663.
13) M. Ghofrani, A. Arabali, M. Etezadi-Amoli, and M.S. Fadali, "A framework for optimal placement of energy storage units within a power system with high wind penetration," *IEEE Trans Sustain Energy*, **4** (*2*) 434–442 (2013). doi:10.1109/TSTE.2012.2227343.
14) A. Soemanto, E. Mohi, M.I. al Irsyad, and Y. Gunawan, "The role of oil fuels on the energy transition toward net zero emissions in indonesia: a policy review," *Evergreen*, **10** (*4*) 2074–2083 (2023). doi:10.5109/7160867.
15) M. Stecca, L.R. Elizondo, T.B. Soeiro, P. Bauer, and P. Palensky, "A comprehensive review of the integration of battery energy storage systems into distribution networks," *IEEE Open Journal of the Industrial Electronics Society*, **1** (*1*) 46–65 (2020). doi:10.1109/OJIES.2020.2981832.
16) A.T. Nguyen, S. Chaitusaney, and A. Yokoyama, "Optimal strategies of siting, sizing, and scheduling of bess: voltage management solution for future lv network," *IEEJ Transactions on Electrical and Electronic Engineering*, **14** (*5*) 694–704 (2019). doi:10.1002/tee.22856.
17) C. H. B. Apribowo, S.P. Hadi, F.D. Wijaya, M. Isnaeni, and B. Setyonegoro, "Optimal allocation of vanadium redox flow battery storage systems with integrated variable renewable energy," *2023 15th International Conference on Information Technology and Electrical Engineering (ICITEE)*, 375–380 (2023). doi:10.1109/ICITEE59582.2023.10317686.
18) A.A. Akhil, G. Huff, A.B. Currier, B.C. Kaun, D.M. Rastler, S.B. Chen, A.L. Cotter, D.T. Bradshaw, and W.D. Gauntlett, "DOE / epri 2013 electricity storage handbook in collaboration with nreca," (*July*) (2013).
19) M.A. Hannan, S.B. Wali, P.J. Ker, M.S.A. Rahman, M. Mansor, V.K. Ramachandaramurthy, K.M. Muttaqi, T.M.I. Mahlia, and Z.Y. Dong, "Battery energy-storage system: a review of technologies, optimization objectives, constraints, approaches, and outstanding issues," *J Energy Storage*, **42** 103023 (2021). doi:10.1016/j.est.2021.103023.
20) C.H.B. Apribowo, Sarjiya, S.P. Hadi, and F.D. Wijaya, "Integration of battery energy storage system to increase flexibility and penetration renewable energy in indonesia: a brief review," *ICPERE 2022 - 5th International Conference on Power Engineering and Renewable Energy, Proceedings*, (2022). doi:10.1109/ICPERE56870.2022.10037530.
21) D. Chattopadhyay, and W. Bank, "BATTERY storage in developing countries: key issues to consider analysis of spot price stochasticity in deregulated wholesale electricity markets view project voltage stability view project," (n.d.). https://www.researchgate.net/publication/330116801 (accessed August 1, 2022).
22) J. Eyer, "Energy storage for the electricity grid : benefits and market potential assessment guide a study for the doe energy storage systems program," (*February*) (2010).
23) M.R. Sheibani, G.R. Yousefi, M.A. Latify, and S. Hacopian, "Energy storage system expansion planning in power systems : a review," 1203–1221 (2018). doi:10.1049/iet-rpg.2018.0089.
24) C.H.B. Apribowo, S. Sarjiya, S.P. Hadi, and F.D. Wijaya, "Optimal planning of battery energy storage systems by considering battery degradation due to ambient temperature: a review, challenges, and new perspective," *Batteries 2022, Vol. 8, Page 290*, **8** (*12*) 290 (2022). doi:10.3390/BATTERIES8120290.
25) Y. Zhang, Z.Y. Dong, F. Luo, Y. Zheng, K. Meng, and K.P. Wong, "Optimal allocation of battery energy storage systems in distribution networks with high wind power penetration," *IET Renewable Power Generation Research*, **10** (*8*) 1105–1113 (2016). doi:10.1049/iet-rpg.2015.0542.
26) N. Kumari, S.K. Singh, and S. Kumar, "MATLAB-based simulation analysis of the partial shading at different locations on series-parallel pv array configuration," *Evergreen*, **09** (*04*) 1126-1139 (2022). doi:10.5109/6625724
27) P.M. de Quevedo, G. Muñoz-delgado, and J. Contreras, "Impact of electric vehicles on the expansion planning of distribution systems considering charging stations," *IEEE Trans Smart Grid*, **10** (*1*) 794–804 (2019).
28) M.A. Hannan, M. Faisal, P. Jern Ker, R.A. Begum, Z.Y. Dong, and C. Zhang, "Review of optimal methods and algorithms for sizing energy storage systems to achieve decarbonization in microgrid applications," *Renewable and Sustainable Energy Reviews*, **131** 110022 (2020). doi:10.1016/J.RSER.2020.110022.
29) K. Fajar, A. Sukra, K. Fajar, A. Sukra, A. Sukmono, L. Shalahuddin, and M.P. Helios, "Effects of battery

state of charge on fuel economy of hybrid electric vehicles : an analysis using the un ece r101 method effects of battery state of charge on fuel economy of hybrid electric vehicles : an analysis using the un ece r101 method," **10** (*3*) 1770–1775 (2023).

30) C.H. Brillianto Apribowo, S.P. Hadi, F.D. Wijaya, M.I. Bambang Setyonegoro, and Sarjiya, "Early prediction of battery degradation in grid-scale battery energy storage system using extreme gradient boosting algorithm," *Results in Engineering*, **21** 101709 (2024). doi:10.1016/J.RINENG.2023.101709.
31) Y. Yang, S. Bremner, C. Menictas, and M. Kay, "Battery energy storage system size determination in renewable energy systems: a review," *Renewable and Sustainable Energy Reviews*, **91** 109–125 (2018). doi:10.1016/j.rser.2018.03.047.
32) T. Bowen, I. Chernyakhovskiy, and P. Denholm, "Grid-scale battery storage: frequently asked questions," *Nrel*, (*2013*) 1–8 (2018). www.greeningthegrid.org.
33) R. Khezri, A. Mahmoudi, and H. Aki, "Optimal planning of solar photovoltaic and battery storage systems for grid-connected residential sector: review, challenges and new perspectives," *Renewable and Sustainable Energy Reviews*, **153** 111763 (2022). doi:10.1016/j.rser.2021.111763.
34) M. Reza, and A. Putra, "Heat management on lifepo4 battery pack for eddy current brake energy storage on rapid braking processes," *Evergreen*, **9** (*2*) 451–456 (2022). doi:10.5109/4794171
35) T. Steckel, A. Kendall, and H. Ambrose, "Applying levelized cost of storage methodology to utility-scale second-life lithium-ion battery energy storage systems," *Appl Energy*, **300** (*July*) (2021). doi:10.1016/j.apenergy.2021.117309.
36) N. Horesh, C. Quinn, H. Wang, R. Zane, M. Ferry, S. Tong, and J.C. Quinn, "Driving to the future of energy storage: techno-economic analysis of a novel method to recondition second life electric vehicle batteries," *Appl Energy*, **295** (*April*) (2021). doi:10.1016/j.apenergy.2021.117007.
37) S. Chai, N.Z. Xu, M. Niu, K.W. Chan, C.Y. Chung, H. Jiang, and Y. Sun, "An evaluation framework for second-life ev/phev battery application in power systems," *IEEE Access*, **9** 152430–152441 (2021). doi:10.1109/ACCESS.2021.3126872.
38) E. Martinez-Laserna, I. Gandiaga, E. Sarasketa-Zabala, J. Badeda, D.I. Stroe, M. Swierczynski, and A. Goikoetxea, "Battery second life: hype, hope or reality? a critical review of the state of the art," *Renewable and Sustainable Energy Reviews*, **93** 701–718 (2018). doi:10.1016/J.RSER.2018.04.035.
39) M.A. Ortega-Vazquez, and D.S. Kirschen, "Estimating the spinning reserve requirements in systems with significant wind power generation penetration," *IEEE Transactions on Power Systems*, **24** (*1*) 114–124 (2009). doi:10.1109/TPWRS.2008.2004745.
40) C.H.B. Apribowo, Sarjiya, S.P. Hadi, and F. Danang Wijaya, "Optimal sizing and siting of battery energy storage systems with retired battery," *ICT-PEP 2022 - International Conference on Technology and Policy in Energy and Electric Power: Advanced Technology for Transitioning to Sustainable Energy and Modern Power Systems, Proceedings*, 327–332 (2022). doi:10.1109/ICT-PEP57242.2022.9988958.
41) A.A.R. Mohamed, R.J. Best, X. Liu, and D. John Morrow, "A comprehensive robust techno-economic analysis and sizing tool for the small-scale pv and bess," *IEEE Transactions on Energy Conversion*, **37** (*1*) 560–572 (2022). doi:10.1109/TEC.2021.3107103.
42) T. Carriere, C. Vernay, S. Pitaval, F.P. Neirac, and G. Kariniotakis, "Strategies for combined operation of pv/ storage systems integrated into electricity markets," *IET Renewable Power Generation*, **14** (*1*) 71–79 (2020). doi:10.1049/iet-rpg.2019.0375.
43) A.A. Kebede, M.S. Hosen, T. Kalogiannis, H.A. Behabtu, M.Z. Assefa, T. Jemal, V. Ramayya, J. Van Mierlo, T. Coosemans, and M. Berecibar, "Optimal sizing and lifetime investigation of second life lithium-ion battery for grid-scale stationary application," *J Energy Storage*, **72** 108541 (2023). doi:10.1016/J.EST.2023.108541.
44) Tumiran, L.M. Putranto, Sarjiya, and E.Y. Pramono, "Maximum penetration determination of variable renewable energy generation: a case in java–bali power systems," *Renew Energy*, **163** 561–570 (2021). doi:10.1016/j.renene.2020.08.048.
45) I. Alsaidan, A. Khodaei, and W. Gao, "A comprehensive battery energy storage optimal sizing model for microgrid applications," *IEEE Transactions on Power Systems*, **33** (*4*) 3968–3980 (2018). doi:10.1109/TPWRS.2017.2769639.
46) Y. Wu, Z. Liu, J. Liu, H. Xiao, R. Liu, and L. Zhang, "Optimal battery capacity of grid-connected pv-battery systems considering battery degradation," *Renew Energy*, **181** 10–23 (2022). doi:10.1016/j.renene.2021.09.036.
47) A.A.R. Mohamed, R.J. Best, X. Liu, and D.J. Morrow, "Residential battery energy storage sizing and profitability in the presence of pv and ev," *2021 IEEE Madrid PowerTech, PowerTech 2021 - Conference Proceedings*, (2021). doi:10.1109/POWERTECH46648.2021.9494792.
48) M. Amini, A. Khorsandi, B. Vahidi, S.H. Hosseinian, and A. Malakmahmoudi, "Optimal sizing of battery energy storage in a microgrid considering capacity degradation and replacement year," *Electric Power Systems Research*, **195** (2021). doi:10.1016/j.epsr.2021.107170.
49) V.V.S.N. Murty, and A. Kumar, "Multi-objective energy management in microgrids with hybrid energy sources and battery energy storage systems,"

Protection and Control of Modern Power Systems, **5** (*1*) 1–20 (2020). doi:10.1186/s41601-019-0147-z.

50) Y. Zhang, Y. Su, Z. Wang, F. Liu, and C. Li, "Cycle-life-aware optimal sizing of grid-side battery energy storage," *IEEE Access*, **9** 20179–20190 (2021). doi:10.1109/ACCESS.2021.3054860.
51) U.G.K. Mulleriyawage, and W.X. Shen, "Impact of demand side management on optimal sizing of residential battery energy storage system," *Renew Energy*, **172** 1250–1266 (2021). doi:10.1016/j.renene.2021.03.122.
52) T. Sayfutdinov, C. Patsios, P. Vorobev, E. Gryazina, D.M. Greenwood, J.W. Bialek, and P.C. Taylor, "Degradation and operation-aware framework for the optimal siting, sizing, and technology selection of battery storage," *IEEE Trans Sustain Energy*, **11** (*4*) 2130–2140 (2020). doi:10.1109/TSTE.2019.2950723.
53) M. Amini, A. Khorsandi, B. Vahidi, S.H. Hosseinian, and A. Malakmahmoudi, "Optimal sizing of battery energy storage in a microgrid considering capacity degradation and replacement year," *Electric Power Systems Research*, **195** (2021). doi:10.1016/j.epsr.2021.107170.
54) I. Alsaidan, A. Khodaei, and W. Gao, "A comprehensive battery energy storage optimal sizing model for microgrid applications," *IEEE Transactions on Power Systems*, **33** (*4*) 3968–3980 (2018). doi:10.1109/TPWRS.2017.2769639.
55) G.S. Georgiou, P. Christodoulides, and S.A. Kalogirou, "Optimizing the energy storage schedule of a battery in a pv grid-connected nzeb using linear programming," *Energy*, **208** 118177 (2020). doi:10.1016/j.energy.2020.118177.
56) Z. Yang, H. Zhong, A. Bose, T. Zheng, Q. Xia, and C. Kang, "A linearized opf model with reactive power and voltage magnitude: a pathway to improve the mw-only dc opf," *IEEE Transactions on Power Systems*, **33** (*2*) 1734–1745 (2018). doi:10.1109/TPWRS.2017.2718551.
57) "Description of case14," (n.d.). https://matpower.org/docs/ref/matpower5.0/case14.html (accessed November 28, 2022).
58) "Power systems test case archive," (n.d.). https://labs.ece.uw.edu/pstca/pf14/pg_tca14bus.htm (accessed November 28, 2022).
59) A.J. Conejo, M. Carrión, and J.M. Morales, "Decision making under uncertainty in electricity markets," **153** (2010). doi:10.1007/978-1-4419-7421-1.
60) NREL, "Solar power data for integration studies | grid modernization," (n.d.).
61) M. Guo, Y. Mu, H. Jia, Y. Deng, X. Xu, and X. Yu, "Electric/thermal hybrid energy storage planning for park-level integrated energy systems with second-life battery utilization," *Advances in Applied Energy*, **4** (*August*) (2021). doi:10.1016/j.adapen.2021.100064.
62) C.A. Rufino Júnior, E. Riva Sanseverino, P. Gallo, D. Koch, Y. Kotak, H.G. Schweiger, and H. Zanin, "Towards a business model for second-life batteries – barriers, opportunities, uncertainties, and technologies," *Journal of Energy Chemistry*, **78** 507–525 (2023). doi:10.1016/j.jechem.2022.12.019.
63) M. Bolinger, S. Weaver, and J. Zuboy, "Is $50/mwh solar for real? falling project prices and rising capacity factors drive utility-scale pv toward economic competitiveness," *Progress in Photovoltaics: Research and Applications*, **23** (*12*) 1847–1856 (2015). doi:10.1002/pip.2630.
64) B. Bai, S. Xiong, B. Song, and M. Xiaoming, "Economic analysis of distributed solar photovoltaics with reused electric vehicle batteries as energy storage systems in china," *Renewable and Sustainable Energy Reviews*, **109** 213–229 (2019). doi:10.1016/J.RSER.2019.03.048.
65) A. Demirci, "Optimal sizing and techno-economic evaluation of microgrids based on 100% renewable energy powered by second-life battery," *IEEE Access*, **11** 113291–113306 (2023). doi:10.1109/ACCESS.2023.3324547.
66) Y. Yaowang Li, Shixu Zhang, Yuliang Liu, Ershun Du, Jun Ye, and N.Z. Li, "Economic analysis of sharing second-life battery for serving multiple wind farms using cloud energy storage model | csee journals & magazine | ieee xplore," *IEEE Access*, (2023).